Solar Fuel Production

DOI: 10.1002/anie.201404953

Photothermal Conversion of CO_2 into CH_4 with H_2 over Group VIII Nanocatalysts: An Alternative Approach for Solar Fuel Production**

Xianguang Meng, Tao Wang, Lequan Liu, Shuxin Ouyang, Peng Li, Huilin Hu, Tetsuya Kako, Hideo Iwai, Akihiro Tanaka, and Jinhua Ye**

Abstract: *The photothermal conversion of CO_2 provides a straightforward and effective method for the highly efficient production of solar fuels with high solar-light utilization efficiency. This is due to several crucial features of the Group VIII nanocatalysts, including effective energy utilization over the whole range of the solar spectrum, excellent photothermal performance, and unique activation abilities. Photothermal CO_2 reaction rates ($mol\,h^{-1}\,g^{-1}$) that are several orders of magnitude larger than those obtained with photocatalytic methods ($\mu mol\,h^{-1}\,g^{-1}$) were thus achieved. It is proposed that the overall water-based CO_2 conversion process can be achieved by combining light-driven H_2 production from water and photothermal CO_2 conversion with H_2. More generally, this work suggests that traditional catalysts that are characterized by intense photoabsorption will find new applications in photo-induced green-chemistry processes.*

How to provide clean, affordable, and reliable energy without causing climate change is a common concern in the world.[1] The conversion of CO_2, the major component of greenhouse gas, into renewable hydrocarbon fuels by solar energy provides a sustainable way for carbon cycling, and is of significance in solving both energy and environmental issues. Today, solar fuel production by CO_2 conversion is mainly achieved according to two approaches: The first approach is based on photocatalytic CO_2 conversion over semiconductors, using photoexcited e^-/h^+ to drive the simultaneous processes of water photooxidation (at the valence band) and CO_2 photoreduction (at the conduction band).[2] However, photocatalytic CO_2 conversion remains very inefficient because of the kinetic limitations of multiple e^-/H^+ transfer processes and the limited abilities of traditional semiconductors to activate thermodynamically stable CO_2 molecules.[3] According to recent results,[2,4] the reaction rates of photocatalytic CO_2 conversion processes using H_2O or H_2 as the hydrogen source are on the order of $\mu mol\,h^{-1}\,g^{-1}$, even leaving aside the uncertainty of the carbon source of the final reduction products (the observed products possibly originate from the photoreforming of residual carbonaceous substances rather than the photoreduction of CO_2). The second approach makes use of the dissociation of CO_2 by two-step thermochemical cycles of metal oxide redox pairs (mainly Zn/ZnO, Ce_2O_3/CeO_2, FeO/Fe_3O_4, and SnO/SnO_2); these cycles are driven by the heat obtained from concentrated solar radiation.[5] However, the very high operation temperature (nearly 2000 °C) and special reactor design are indispensable to realize this reaction. More convenient methods for light-driven CO_2 conversion, especially for water-based CO_2 conversion, a process that mimics photosynthesis, are urgently required.

The recently emerged photothermal effect (or rapid heating) of nanometals inspired us to seek new methods for the production of solar fuels. The photothermal effect of nanometals stems from the dissipation of photon energy into heat. It appears that the remarkable increase in the local temperature of the nanometals results from excitation of the surface plasmon band and the consequential fast thermal relaxation of the exciton, leading to prompt conversion of the light energy into heat.[6] The photothermal effect, which is induced by surface plasmon resonance (SPR) absorption, has been widely studied for applications in cancer therapy (mainly Au and Pd).[7] The SPR-induced charge transfer and/or the photothermal effect also enable the effective harvesting of visible and even near-infrared (NIR) light to drive useful reaction processes, such as water splitting,[8] the decomposition of organic contaminants,[9] and Suzuki coupling reactions.[10] Therefore, we were encouraged to face the great challenge of highly efficient utilization of solar energy (mainly 300–2500 nm, photon energy distributed as follows: ultraviolet light: 4%; visible light: 43%; infrared radiation: 53%). Herein, we expand the use of this photothermal effect to nanocatalysts that are based on Group VIII metals (Ru, Rh, Ni, Co, Pd, Pt, Ir, and Fe) for the catalytic conversion of CO_2 with H_2 into CH_4 (Sabatier reaction) and CO (reverse

[*] X. Meng, Dr. T. Wang, Dr. L. Liu, Dr. S. Ouyang, Dr. P. Li, Dr. T. Kako, Prof. J. Ye
Environmental Remediation Materials Unit and International Center for Materials Nanoarchitectonics (WPI-MANA)
1-1 Namiki, Tsukuba, Ibaraki 305-0044 (Japan)
E-mail: oysx@tju.edu.cn
Jinhua.YE@nims.go.jp
X. Meng, Dr. T. Kako, Prof. J. Ye
Graduate School of Chemical Science and Engineering
Hokkaido University
Sapporo 060-0814 (Japan)
Dr. S. Ouyang, H. Hu, Prof. J. Ye
TU-NIMS Joint Research Center, School of Material Science and Engineering, Tianjin University
92 Weijin Road, Tianjin (P.R. China)
Dr. H. Iwai, Dr. A. Tanaka
Materials Analysis Station
National Institute for Materials Science
1-2-1 Sengen, Tsukuba, Ibaraki 305-0047 (Japan)

[**] We received financial support from the World Premier International Research Center Initiative (WPI Initiative) on Materials Nanoarchitectonics (MANA), MEXT (Japan), and the National Basic Research Program of China (973 Program, 2014CB239301).
Supporting information for this article is available on the WWW under http://dx.doi.org/10.1002/anie.201404953.

water–gas shift reaction) for the highly efficient production of solar fuels. These nanocatalysts are generally of a dark grey or black color (Supporting Information, Figure S1). They have much stronger photoabsorption abilities than traditional semiconductor photocatalysts and display a strong photothermal effect. The results of this work indicate that with Group VIII catalysts, reaction rates for the photothermal CO_2 conversion that are several orders of magnitude higher (ca. mol h^{-1} g^{-1}) than those observed with other photocatalysts can be achieved. The highly efficient CO_2 conversion is due to several features of the Group VIII nanocatalysts, including effective energy utilization over the whole range of the solar spectrum, excellent photothermal performance, and a unique H_2 activation ability (to create active H atoms, which are the key intermediates for CO_2 hydrogenation at low onset temperatures).[11]

Herein, the intentional use of inert Al_2O_3 as the support instead of photocatalytically active materials such as TiO_2 enabled us to independently investigate the performance of the Group VIII nanocatalysts in photothermal CO_2 conversion. The catalysts were prepared by impregnation of mesoporous Al_2O_3 (BET surface area = 136 m^2 g^{-1}; see Figure S2) in the precursor solutions of Group VIII metals, followed by calcination at 300 °C for two hours. Further reduction by H_2 was needed for the Ni/Al_2O_3, Co/Al_2O_3, and Fe/Al_2O_3 catalysts (for TEM images of the Group VIII nanocatalysts on Al_2O_3 support, see Figure S3; the particle size of the Group VIII nanocatalysts varied from several nanometers to several tens of nanometers). CO_2 (ca. 2–2.05 mmol) and H_2 (ca. 8.2–8.5 mmol; the molar H_2/CO_2 ratio is slightly larger than 4:1) were mixed as the initial reactants in a batch-type reaction system (Figure S20).

Under photoirradiation, all of the Group VIII nanoparticles were active catalysts for CO_2 conversion (Figure 1 a for the Ru/Al_2O_3 catalyst; for the other catalysts, see Figure S4). Their activities and selectivities are summarized in Table 1. The use of Ru/Al_2O_3 and Rh/Al_2O_3 led to the highest reaction rates, followed by the two cost-efficient catalysts Ni/Al_2O_3 and Co/Al_2O_3. The performance of the Ru/Al_2O_3, Rh/Al_2O_3, Ni/Al_2O_3, Co/Al_2O_3, and Pd/Al_2O_3 catalysts was superior to that of the Pt/Al_2O_3, Ir/Al_2O_3, and Fe/Al_2O_3 catalysts in terms of selectivity for CH_4 production (ca. 99%) and CO_2 conversion (>90%). Only a very small amount of CO was produced by pure Al_2O_3 in control experiments (Figure S4 o and Figure S5). In the absence of H_2, photothermal CO_2 conversion cannot occur (Figure S6). Therefore, both the Group VIII catalysts and H_2 are indispensable for highly efficient photothermal CO_2 conversion. As the cheapest noble metal among the Group VIII metals, the Ru nanocatalyst displayed excellent recycling properties (Figure S7). No obvious changes were observed with respect to nanoparticle size and distribution for the Ru as well as Ni nanoparticles after photothermal reactions (Figure S3 a–d). The fast decay of the performance of the Pt/Al_2O_3 catalyst in CO_2 conversion is possibly due to a poisoning effect induced by CO.[12] Under photoirradiation, the maximum reaction rates for the conversion of CO_2 in the presence of Group VIII catalysts were measured to be in the magnitude of mol h^{-1} g^{-1} (the carbon source for CH_4 produced over the Ni/Al_2O_3 catalyst was confirmed by labelling experiments with $^{13}CO_2$; Figure S8). For the current

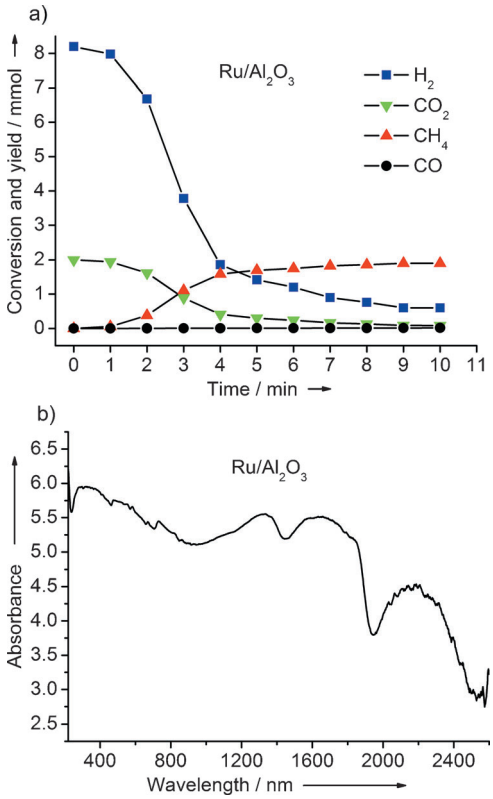

Figure 1. a) Photothermal CO_2 conversion with and b) UV/Vis/NIR spectrum of the Ru/Al_2O_3 catalyst. The reaction was performed in a gas mixture of CO_2 (ca. 2–2.05 mmol) and H_2 (ca. 8.2–8.5 mmol) under irradiation with a 300 W Xenon lamp. The catalyst sample (0.1 g) was spread onto a round air-permeable quartz fiber filter with an area of 7 cm^2.

Table 1: Activities and selectivities of the Group VIII catalysts.[a]

Sample	Metal loading[b] [wt%]	R_{max}[c] [mol h^{-1} g^{-1}]	Conversion[d] of CO_2 [%]	Selectivity[d] for CH_4 [%]	Selectivity[d] for CO [%]
Ru/Al_2O_3	2.4	18.16	95.75	99.22	0.78
Rh/Al_2O_3	2.6	6.36	96.25	99.48	0.52
Ni/Al_2O_3	2.1	2.30	93.25	99.04	0.95
Co/Al_2O_3	2.5	0.90	92.58	99.51	0.49
Pd/Al_2O_3	2.0	0.53	93.43	98.64	1.36
Pt/Al_2O_3	2.4	0.47	60.42	15.55	84.45
Ir/Al_2O_3	2.8	0.05	14.94	63.25	36.74
Fe/Al_2O_3	2.4	0.02	7.27	4.04	95.96
TiO_2	–	9.04×10^{-7}	–	68.23	31.77
Pt/TiO_2[e]	2.5	8.01×10^{-9}	–	100	0
Ru/TiO_2[e]	2.5	5.31×10^{-9}	–	100	0

[a] For the reaction conditions, see Figure 1 a. [b] Loading amounts of the Group VIII nanoparticles determined by ICP-OES. [c] R_{max}: the maximum CO_2 reaction rate. [d] Based on the amount of the gas at the end of the reaction (for the reaction duration, see Figures 1 a, S4 a, and S9 a,b). [e] Water (2 mL) was used instead of H_2 as the hydrogen source.

CO_2 conversion by a photocatalytic method using H_2O or H_2 as the hydrogen source, reaction rates that are only on the order of $\mu mol\,h^{-1}\,g^{-1}$ or even $nmol\,h^{-1}\,g^{-1}$ have been described.[2,4] In comparative experiments with a high-surface-area TiO_2 photocatalyst (commercial ST01, BET surface area = $343\ m^2\,g^{-1}$) for the CO_2 conversion in the presence of H_2 (Figure S9a) or H_2O (Ru or Pt as co-catalysts; Figure S9b) under the same photoirradiation conditions, CO_2 reaction rates on the order of $nmol\,h^{-1}\,g^{-1}$ to $\mu mol\,h^{-1}\,g^{-1}$ were obtained (Table 1). Therefore, the CO_2 reaction rates that are achieved by the Group VIII catalysts through photothermal activation are approximately six orders of magnitude greater than those achieved with photocatalytic methods. A valence-state analysis of some primary Group VIII nanocatalysts (Ru, Rh, and Ni) showed that the active phase should mainly consist of metallic species (for details of the XPS analysis, see Figure S10).

UV/Vis/NIR spectra indicate that all of the Group VIII catalysts are excellent absorbers over a very broad photoirradiation range that covers ultraviolet light, visible light, and infrared radiation (Figure 1b for the Ru/Al_2O_3 catalyst; for the other catalysts, see Figure S4). The intense absorption implies that a high utilization efficiency of solar energy would be feasible. Monitoring of the catalyst temperature demonstrated that the photoirradiation induced a significant thermal effect (Figure 2 and Figure S11). For almost all of the

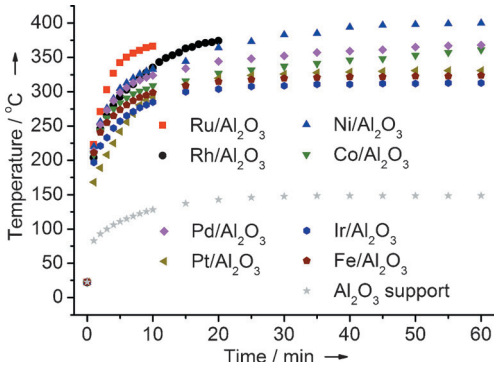

Figure 2. Monitoring of the catalyst temperature.

catalysts, the temperature reached approximately 200 °C within the first minute, whereas the temperature of pure Al_2O_3 support in a control experiment was measured to be approximately 80 °C. Under continuous photoirradiation, Group VIII catalysts maintain a reaction temperature of about 300–400 °C, which is approximately 200 °C higher than that of pure Al_2O_3 support. The excellent photothermal properties in conjunction with the unique activation ability of the Group VIII nanocatalysts favor the highly efficient photo-induced conversion of CO_2. No additional enhancement effects on the CO_2 conversion that are due to the irradiation were observed. We then compared the CH_4 evolution over the Ru/Al_2O_3 catalyst under thermal and photothermal conditions (Figure S12). In both experiments, the onset temperatures were found to be approximately 140 °C. No obvious differences between the CH_4 evolution curves for the two sets of conditions were found. To investigate whether CO_2 hydrogenation is affected by photocatalytic processes (photoexcitation processes), the CH_4 evolution over the Ru/Al_2O_3 catalyst was measured under irradiation with monochromatic light. With this method, the thermal effect was effectively suppressed (no obvious temperature increase was observed, and the temperature remained at ca. 21–23 °C over the whole experiment). We selected some typical monochromatic light filters (441, 502, 549, 601, and 710 nm) in the visible-light range for this test (for the photon distribution, see Figure S13a). It was found that the CH_4 evolution rate (CO evolution was not observed) was very low (ca. 0.02 μmol/100 min) in the dark, and this evolution rate remained almost unchanged no matter which monochromatic light was used (Figure S13b). This result reflects the fact that photo-induced CO_2 methanation over Ru/Al_2O_3 is not mediated by photocatalysis, but by a photothermal effect. All of these results imply that the mechanism of this process differs from the alleged photocatalytic mechanism,[13] and that the light-induced thermal effect should dominate the process of CO_2 conversion.

Wide-band-gap semiconductors ($E_g > 3$ eV), such as Ti-, Nb-, Ta-, Ga-, and Ge-based oxides with adequate redox potentials, constitute the main materials for photocatalytic CO_2 conversion, which are highly dependent upon excitation by ultraviolet irradiation (which only accounts for 4% of the total solar energy).[2] In contrast to traditional photocatalytic methods, the photothermal CO_2 conversion over Group VIII catalysts does not require ultraviolet irradiation as the excellent absorption of visible light and infrared radiation (which together account for 96% of the total solar energy) can effectively drive photothermal CO_2 conversion. In the absence of ultraviolet light, photothermal CO_2 conversion can still proceed over the Ru/Al_2O_3 catalyst (Figure S14). Therefore, Group VIII catalysts are advantageous over traditional photocatalysts because of the highly efficient utilization of solar energy and in particular of the low-energy photons of visible light and infrared radiation.

It is interesting that the low-cost Ni/Al_2O_3 catalyst was even more active than some noble-metal catalysts (Pd, Pt, and Ir). This implies that the Ni/Al_2O_3 catalyst is a promising candidate for practical use in future artificial photo-induced CO_2 conversion systems. In further investigations, increasing the loading amount of Ni on Al_2O_3 (for XRD and TEM results, see Figure S15, S16) demonstrated that a 7.3 wt% Ni/Al_2O_3 catalyst achieved comparable activity to a 2.6 wt% Rh/Al_2O_3 catalyst, and CO_2 conversion reached 90% within 15 minutes (Figure 3a and Figure S4a). Both temperature variation and CO_2 conversion showed similar tendency when increasing the loading amount of Ni. (Figure 3). Obviously, more catalytically active sites and heat-gathering centers will be created with an increase in the amount of Ni on the Al_2O_3 support, which leads to remarkably enhanced CO_2 conversion. Aside from the catalytic abilities of the nanometals, some other factors (mainly the design of the reactor) interfered with the increase in CO_2 conversion efficiency with an increasing in the loading amount of Ni from 7.3% to 12.9%. For example, the gas flow rate (controlled by the vibration of the gas circulation pump; Figure S20) has

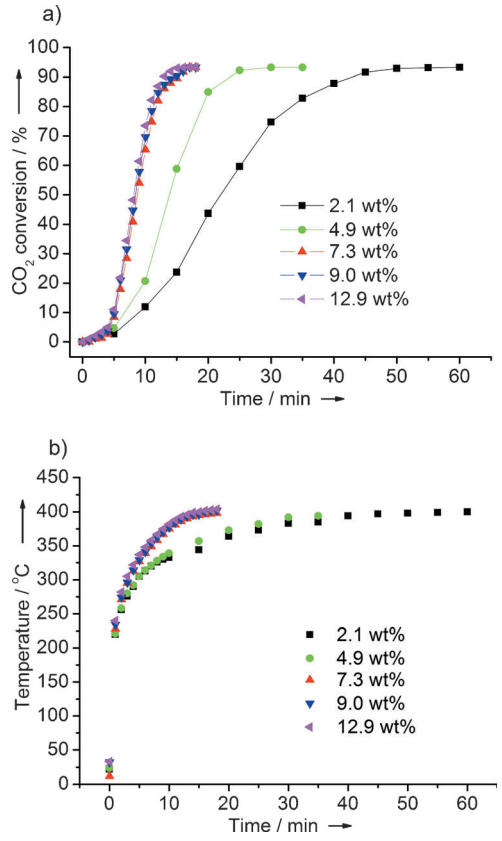

Figure 3. a) CO_2 conversion with and b) temperature monitoring of Ni/Al_2O_3 catalysts. For the reaction conditions, see Figure 1 a.

reached its maximum for the present batch-type reaction system. Although increasing the loading amount of Ni will lead to an increase in the number of catalytically active sites, the limited flow rate restricts the amount of reactant gas that can be supplied and thus hampers the increase in the reaction rate of CO_2 conversion. However, the reaction speed of CO_2 conversion might be further increased by using a different reaction system (such as a flow-type reaction system). The use of Ni/Al_2O_3 catalysts with larger Ni particle sizes (ca. 20–100 nm, obtained from the H_2 reduction of Al_2O_3 supported NiO nanoparticles produced by ball milling) led to a slight decrease in reaction temperature as well as CO_2 conversion (Figure S17). This might be caused by the change in photothermal conversion owing to the different size of the Ni particles and the decrease in the number of catalytically active sites. Using commercial TiO_2 (P25, BET surface area = 57 $m^2 g^{-1}$) as a support remarkably enhanced CO_2 conversion with Ni nanocatalysts (Figure S18). This support effect should be the subject of future studies.

Ideally, CO_2 conversion should mimic the photosynthesis of green plants by using abundant and stable H_2O instead of H_2 as the hydrogen source for CO_2 conversion to realize the sustainable production of solar fuels and to maximize the conversion of solar energy into chemical energy. However, photocatalytic CO_2 conversion is far less efficient in terms of reaction rates and the efficient utilization of solar energy. Future studies on water-based CO_2 conversion and solar fuel production should be based on more flexible strategies for solar-energy utilization than photocatalysis. Based on the results of this work, we propose that water-based solar fuel generation can be achieved by a two-step process [Eq. (1)–(3)], which combines photo-driven H_2 production through

$$\text{Step 1}: \quad 2H_2O \rightarrow 2H_2 + O_2 \tag{1}$$

$$\text{Step 2}: \quad 4H_2 + CO_2 \rightarrow CH_4 + 2H_2O \tag{2}$$

$$\text{Overall process}: \quad CO_2 + 2H_2O \rightarrow 2O_2 + CH_4 \tag{3}$$

water splitting and photothermal CO_2 hydrogenation (Figure 4). H_2 production could be realized through different

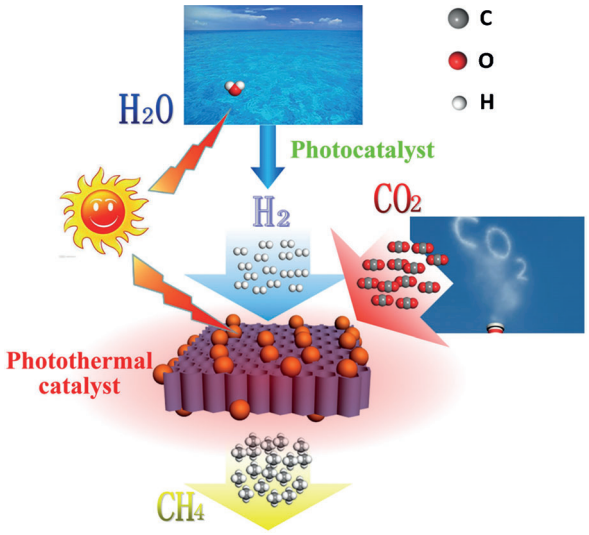

Figure 4. Two-step water-based CO_2 conversion driven by solar energy.

light-driven methods, including photocatalysis,[14] photoelectrochemistry,[15] photothermal effects,[5a,b,16] and photobiology.[17] Then, the generated H_2 will be used as a hydrogen source for photothermal CO_2 methanation. For example, according to recent results on the photocatalytic production of H_2 through water splitting in the absence/presence of a sacrificial reagent, the H_2 evolution rate is on the order of $\mu mol\,h^{-1}\,g^{-1}$ to $mmol\,h^{-1}\,g^{-1}$.[14d] Given that all of the H_2 was used for photothermal CO_2 conversion, the overall reaction rate for two-step water-based CO_2 conversion can still be expected to be higher than that of the direct CO_2 photoreduction by water over semiconductor photocatalysts. Therefore, the two-step method should become more efficient and technically feasible in the future. After combustion of CH_4 (the primary component of compressed natural gas), the generated CO_2 can be recycled[18] for continuous methanation. In theory, zero carbon dioxide emission can be realized if a rationally designed carbon cycling system can be implemented (Figure S19).

In summary, the outstanding CO_2 conversion efficiency highlighted herein is based on two predominant features of the Group VIII nanocatalysts, namely 1) the highly efficient utilization of solar light and excellent photothermal performance, and 2) a unique activation ability for the hydro-

genation of CO_2. The progress in the development of technologies for the light-driven H_2 production through water splitting and the highly efficient photothermal CO_2 hydrogenation reported herein illustrate the feasibility of overall water-based CO_2 conversion. It should be noted that catalytic CO_2 hydrogenation covers a wide range of reaction processes. Aside from the production of solar fuels, hydrogenation of CO_2 can also produce other useful chemical feedstocks.[19] Future work should focus on exploring diversified reaction pathways for photothermal CO_2 conversion. Studies of photothermal catalysis in general and new reaction mechanisms as well as of potential synergism between light and thermal effects, in particular, will create new opportunities for chemical science and technology.

Received: May 4, 2014
Published online: July 17, 2014

Keywords: carbon dioxide · hydrogenation · photothermal effects · solar fuels · transition metals

[1] S. Chu, A. Majumdar, *Nature* **2012**, *488*, 294 – 303.
[2] a) S. N. Habisreutinger, L. Schmidt-Mende, J. K. Stolarczyk, *Angew. Chem.* **2013**, *125*, 7516 – 7557; *Angew. Chem. Int. Ed.* **2013**, *52*, 7372 – 7408; b) S. Navalón, A. Dhakshinamoorthy, M. Álvaro, H. Garcia, *ChemSusChem* **2013**, *6*, 562 – 577; c) S. Yan, J. Wang, H. Gao, N. Wang, H. Yu, Z. Li, Y. Zhou, Z. Zou, *Adv. Funct. Mater.* **2013**, *23*, 1839 – 1845; d) K. Teramura, S. Iguchi, Y. Mizuno, T. Shishido, T. Tanaka, *Angew. Chem.* **2012**, *124*, 8132 – 8135; *Angew. Chem. Int. Ed.* **2012**, *51*, 8008 – 8011.
[3] V. P. Indrakanti, J. D. Kubicki, H. H. Schobert, *Energy Environ. Sci.* **2009**, *2*, 745 – 758.
[4] a) Y. Kohno, H. Ishikawa, T. Tanaka, T. Funabiki, S. Yoshida, *Phys. Chem. Chem. Phys.* **2001**, *3*, 1108 – 1113; b) K. Teramura, T. Tanaka, H. Ishikawa, Y. Kohno, T. Funabiki, *J. Phys. Chem. B* **2003**, *107*, 346 – 354; c) K. Teramura, S.-i. Okuoka, H. Tsuneoka, T. Shishido, T. Tanaka, *Appl. Catal. B* **2010**, *96*, 565 – 568; d) N. Ahmed, M. Morikawa, Y. Izumi, *Catal. Today* **2012**, *185*, 263 – 269.
[5] a) W. C. Chueh, C. Falter, M. Abbott, D. Scipio, P. Furler, S. M. Haile, A. Steinfeld, *Science* **2010**, *330*, 1797 – 1801; b) A. Stamatiou, P. G. Loutzenhiser, A. Steinfeld, *Chem. Mater.* **2009**, *21*, 851 – 859; c) S. Abanades, M. Chambon, *Energy Fuels* **2010**, *24*, 6667 – 6674; d) L. J. Venstrom, R. M. De Smith, Y. Hao, S. M. Haile, J. H. Davidson, *Energy Fuels* **2014**, *28*, 2732 – 2742.
[6] a) A. Primo, A. Corma, H. Garcia, *Phys. Chem. Chem. Phys.* **2011**, *13*, 886 – 910; b) A. Takami, H. Kurita, S. Koda, *J. Phys. Chem. B* **1999**, *103*, 1226 – 1232.
[7] a) Y. Xiong, Y. Xia, *Adv. Mater.* **2007**, *19*, 3385 – 3391; b) M. S. Yavuz, Y. Cheng, J. Chen, C. M. Cobley, Q. Zhang, M. Rycenga, J. Xie, C. Kim, K. H. Song, A. G. Schwartz, L. V. Wang, Y. Xia, *Nat. Mater.* **2009**, *8*, 935 – 939; c) X. Huang, S. Tang, X. Mu, Y. Dai, G. Chen, Z. Zhou, F. Ruan, Z. Yang, N. Zheng, *Nat. Nanotechnol.* **2011**, *6*, 28 – 32; d) L. C. Kennedy, L. R. Bickford, N. A. Lewinski, A. J. Coughlin, Y. Hu, E. S. Day, J. L. West, R. A. Drezek, *Small* **2011**, *7*, 169 – 183; e) Y. Su, X. Wei, F. Peng, Y. Zhong, Y. Lu, S. Su, T. Xu, S.-T. Lee, Y. He, *Nano Lett.* **2012**, *12*, 1845 – 1850; f) J. Tang, X. Jiang, L. Wang, H. Zhang, Z. Hu, Y. Liu, X. Wu, C. Chen, *Nanoscale* **2014**, *6*, 3670 – 3678; g) J.-W. Xiao, S.-X. Fan, F. Wang, L.-D. Sun, X.-Y. Zheng, C.-H. Yan, *Nanoscale* **2014**, *6*, 4345 – 4351.
[8] a) S. Mubeen, J. Lee, N. Singh, S. Kramer, G. D. Stucky, M. Moskovits, *Nat. Nanotechnol.* **2013**, *8*, 247 – 251; b) J. B. Priebe, M. Karnahl, H. Junge, M. Beller, D. Hollmann, A. Brückner, *Angew. Chem.* **2013**, *125*, 11631 – 11635; *Angew. Chem. Int. Ed.* **2013**, *52*, 11420 – 11424.
[9] a) L. Liu, S. Ouyang, J. Ye, *Angew. Chem.* **2013**, *125*, 6821 – 6825; *Angew. Chem. Int. Ed.* **2013**, *52*, 6689 – 6693; b) X. Chen, H.-Y. Zhu, J.-C. Zhao, Z.-F. Zheng, X.-P. Gao, *Angew. Chem.* **2008**, *120*, 5433 – 5436; *Angew. Chem. Int. Ed.* **2008**, *47*, 5353 – 5356.
[10] a) F. Wang, C. Li, H. Chen, R. Jiang, L.-D. Sun, Q. Li, J. Wang, J. C. Yu, C.-H. Yan, *J. Am. Chem. Soc.* **2013**, *135*, 5588 – 5601; b) X. Huang, Y. Li, Y. Chen, H. Zhou, X. Duan, Y. Huang, *Angew. Chem.* **2013**, *125*, 6179 – 6183; *Angew. Chem. Int. Ed.* **2013**, *52*, 6063 – 6067.
[11] a) T. Abe, M. Tanizawa, K. Watanabe, A. Taguchi, *Energy Environ. Sci.* **2009**, *2*, 315 – 321; b) S. Eckle, H.-G. Anfang, R. J. Behm, *J. Phys. Chem. C* **2011**, *115*, 1361 – 1367; c) E. Vesselli, J. Schweicher, A. Bundhoo, A. Frennet, N. Kruse, *J. Phys. Chem. C* **2011**, *115*, 1255 – 1260.
[12] Q. Li, R. He, J.-A. Gao, J. O. Jensen, N. J. Bjerrum, *J. Electrochem. Soc.* **2003**, *150*, A1599 – A1605.
[13] F. Sastre, A. V. Puga, L. Liu, A. Corma, H. García, *J. Am. Chem. Soc.* **2014**, *136*, 6798 – 6801.
[14] a) Z. Zou, J. Ye, K. Sayama, H. Arakawa, *Nature* **2001**, *414*, 625 – 627; b) K. Maeda, K. Teramura, D. Lu, N. Saito, Y. Inoue, K. Domen, *Angew. Chem.* **2006**, *118*, 7970 – 7973; *Angew. Chem. Int. Ed.* **2006**, *45*, 7806 – 7809; c) T.-F. Yeh, C.-Y. Teng, S.-J. Chen, H. Teng, *Adv. Mater.* **2014**, *26*, 3297 – 3303; d) A. Kudo, Y. Miseki, *Chem. Soc. Rev.* **2009**, *38*, 253 – 278; e) H. Tong, S. Ouyang, Y. Bi, N. Umezawa, M. Oshikiri, J. Ye, *Adv. Mater.* **2012**, *24*, 229 – 251; f) K. Chang, Z. Mei, T. Wang, Q. Kang, S. Ouyang, J. Ye, *ACS Nano* **2014**, DOI: 10.1021/nn5019945.
[15] a) S. D. Tilley, M. Cornuz, K. Sivula, M. Grätzel, *Angew. Chem.* **2010**, *122*, 6549 – 6552; *Angew. Chem. Int. Ed.* **2010**, *49*, 6405 – 6408; b) M. G. Walter, E. L. Warren, J. R. McKone, S. W. Boettcher, Q. Mi, E. A. Santori, N. S. Lewis, *Chem. Rev.* **2010**, *110*, 6446 – 6473.
[16] T. Kodama, N. Gokon, *Chem. Rev.* **2007**, *107*, 4048 – 4077.
[17] M. L. Ghirardi, A. Dubini, J. Yu, P.-C. Maness, *Chem. Soc. Rev.* **2009**, *38*, 52 – 61.
[18] M. E. Boot-Handford, J. C. Abanades, E. J. Anthony, M. J. Blunt, S. Brandani, N. Mac Dowell, J. R. Fernandez, M.-C. Ferrari, R. Gross, J. P. Hallett, R. S. Haszeldine, P. Heptonstall, A. Lyngfelt, Z. Makuch, E. Mangano, R. T. J. Porter, M. Pourkashanian, G. T. Rochelle, N. Shah, J. G. Yao, P. S. Fennell, *Energy Environ. Sci.* **2014**, *7*, 130 – 189.
[19] a) A. Tlili, X. Frogneux, E. Blondiaux, T. Cantat, *Angew. Chem.* **2014**, *126*, 2577 – 2579; *Angew. Chem. Int. Ed.* **2014**, *53*, 2543 – 2545; b) W. Wang, S. Wang, X. Ma, J. Gong, *Chem. Soc. Rev.* **2011**, *40*, 3703 – 3727; c) X. Xu, J. A. Moulijn, *Energy Fuels* **1996**, *10*, 305 – 325.

